# When Heating Isn't Cooling in Reverse: Nosé-Hoover Thermostat Fluctuations from Equilibrium Symmetry to Nonequilibrium Asymmetry

Hesam Arabzadeh<sup>1</sup> and Brad Lee Holian<sup>2</sup>

<sup>1)</sup>Department of Chemistry, University of Missouri, Columbia, Missouri 65211, USA

<sup>2)</sup>Theoretical Division, Los Alamos National Laboratory, Los Alamos, New Mexico 87545, USA

(\*Electronic mail: blhksh@gmail.com)

(Dated: 30 October 2025)

Recent laboratory experimental work has suggested that heating and cooling processes may exhibit intrinsic asymmetry, with heating occurring more efficiently than cooling. Two decades earlier, molecular dynamics simulations addressed the topic of heating one side of a computational cell while cooling the other side by applying two different thermostats. We revisit those computer calculations, recapitulating the underlying theory, and showing how we might have been able to predict the lab results from tantalizing partial MD results. Recent realizations of a simple two-dimensional one-particle cell model gave surprisingly relevant results, by thermostatting the two directions (x and y) at two different temperatures: at equilibrium, the thermostatting variables in each direction were identical, while under nonequilibrium temperature differences, the heating variable was weaker than the cooling one. At the same time, MD simulations from four decades ago by Evans and Holian piqued our curiosity, since they had reported a surprising skew in the Nosé–Hoover thermostat variable  $\xi$  under equilibrium conditions – indicating a statistical bias in energy injection versus extraction. In this study, we revisit those results using modern MD simulations of a Lennard-Jones soft-sphere fluid with exact reproduction of their setup. We show that when (1) center-of-mass velocity is set to zero, (2) the equations of motion are carefully integrated by finite central differencing, and (3) sampling time is sufficiently long, the distribution of  $\xi$  is symmetric and Gaussian with zero mean, as predicted by theory and convincingly validated by error estimates using two approaches. We then demonstrate clear asymmetry in the distribution of both thermostat variables for the simple cell model: the cold bath requires significantly stronger damping than the hot bath requires anti-damping – matching an exact analytic relation  $\langle \xi_x \rangle / \langle \xi_y \rangle = -T_y / T_x$ , linking thermostat effort to thermal bias and showing how this is related to the negative rate of change in the entropy of the system, accompanying the contraction of phase space onto a fractal strange attractor of lower dimension. Our results clearly identify the microscopic origin of heating-cooling asymmetry as a genuine nonequilibrium effect, thereby strongly confirming the results of laboratory experiments.

#### I. INTRODUCTION

"C'est la dissymétrie qui crée le phénomène."

(It is the asymmetry that creates the phenomenon.)

-Pierre Curie, Journal de Physique 3, 393 (1894)

The laws of thermodynamics are generally assumed to treat heating and cooling on equal footing. Microscopic time-reversibility implies that energy can, in principle, be injected or removed with equivalent ease, subject only to fluctuations. Yet recent experiments have cast doubt on this intuitive symmetry. Ibáñez et al. demonstrated that heating a system occurs more efficiently – faster and with less dissipation – than cooling the same system by the same amount.

The Ibáñez et al. heating and cooling experiments<sup>1</sup> were conducted on colloidal particles (silica microspheres of diameter one micrometer) with charged surfaces, suspended in water, confined by a near-infrared laser trap, and subjected to a heat bath produced by a white noise electric field. Particle Brownian motion was tracked by laser scattering for three temperature quench protocols, i.e., relaxation between either a higher temperature or lower to an intermediate target temperature, then the reverse procedure starting from equilibration at the target temperature, and finally, either heating or cooling between only two temperatures. In all cases, heating is seen to be more easily accomplished than cooling when a nonequilibrium temperature difference exists; otherwise, at equilibrium, there is no bias. This nonequilibrium asymmetry raises important questions: Is the asymmetry in heating and cooling a purely macroscopic effect? Or does it emerge naturally at the microscopic scale?

One of us (BLH) recalled, upon seeing the Ibáñez results, that Evans and Holian<sup>2</sup>, in a 1985 molecular-dynamics (MD) computer simulation of a Nosé–Hoover (NH) thermostatted fluid, observed a similar asymmetry favoring heating – but at equilibrium! The NH thermostat<sup>3</sup> modifies the atomistic Newtonian equations of motion by introducing an integral feedback term (the negative of a thermostatting-rate variable  $\xi$  times particle velocity) into the momentum rate of change. The Nosé–Hoover thermostat behaves like a heat bath, represented by  $\xi$ , an additional phase-space degree of freedom outside the normal particle degrees of freedom (coordinates and momenta). When the thermostat coefficient  $\xi$  is positive, the thermostat heat bath takes energy out of all particles by slowing them down (frictional); when  $\xi$  is negative, the thermostat pumps energy into the particles, speeding them up (anti-frictional); at equilibrium,  $\xi$  fluctuates around zero. NH thermostatting at equilibrium makes the fluid behave as though it were sampling the NVT canonical

ensemble (N particles in volume V and temperature T). The asymmetry observed<sup>2</sup> in the distribution of  $\xi$ , skewed toward negative values (favoring heating), were considered remarkable, since theory predicts a zero mean.

By Fourier's Law, heat flows irreversibly "downhill" from a hot temperature  $T_1$  to a cold temperature  $T_0$  with  $T_1 > T_0$ . We have just recently studied the two-dimensional single-particle cell model<sup>4</sup>, where a wanderer particle moves in a periodic box with confinement provided by repulsive "mounds" at the four corners, and temperature in the two directions are orthogonally thermostatted by Nosé–Hoover: one direction hot (x) at temperature  $T_1 = T_x$  and one cold (y) at  $T_0 = T_y$ . This cell model displayed the same asymmetry in the Lyapunov spectrum under nonequilibrium conditions as it does for the two thermostatting coefficients,  $\xi_0$  and  $\xi_1$ , but no sign of asymmetry at all when  $T_x = T_y$ . Thus, we were prompted by these results to revisit the Evans and Holian equilibrium MD simulation, to see if modern MD could confirm the old apparent asymmetry.

In 2002, a many-body nonequilibrium molecular-dynamics (NEMD) simulation of heat flow<sup>5</sup> was inspired by an imaginary thought experiment: a Maxwell Demon separates a hot reservoir at temperature  $T^{(1)}$  (steady-state average is  $T_1 > T_0$ ) from a cold sample at temperature  $T^{(0)}$  (steadystate average is  $T_0$ ), using an invisible wall; sample and reservoir particles interact across the boundary at x = 0 by terms in the total potential energy  $\Phi$ . Particles can move freely between the two sides and are subject to periodic boundary conditions (PBC). The Demon applies two Nosé-Hoover thermostats: for any sample particle at x < 0, the rate is  $\xi_0$ , whose long-time average is positive, so as to extract heat from the cold sample; for any reservoir particle at x > 0, the rate is  $\xi_1$ , whose long-time average is negative, so as to pump heat into the hot reservoir. Let us assume that there are an equal number of particles, N on average, in both the hot reservoir and cold sample. Of course, the temperature profile smoothes out to become approximately sinusoidal, which allows the resulting simulation, with decreasing temperature difference, to be analyzed by Navier-Stokes-Fourier hydrodynamics to yield the thermal conductivity at the Green-Kubo (equilibrium) limit. (Similarly, shear viscosity can be obtained from a system where one side has a fluid velocity in the y-direction imposed by a fluctuating acceleration, while the other has the opposite driving; in this case, only one NH thermostat keeps the temperature constant on both sides; it's the velocity profile that smoothes out to be nearly sinusoidal.)

The example chosen for NEMD in Ref.<sup>5</sup> was an extreme case of heat flow, namely, a cold solid next to a hot fluid, with a melted interface. The resulting fluid thermal conductivity at the interface was somewhat higher than the Green–Kubo limit, but not by much. The steady-state positive

value of  $\xi_0$  for the cold sample was reported; unfortunately, the paper gave no clue about the magnitude of the negative coefficient for pumping heat into the hot side – a missed opportunity! Nevertheless, this Demonic NEMD thought experiment allows us to make some general arguments about the entropic origin of the asymmetry of nonequilibrium heating versus cooling.

Focusing on one side or the other of the Maxwell Demon system, the volume V contains N atoms, characterized by the flow velocity of the center-of-mass (CM). Subtracting out that CM velocity results in what is called the "peculiar" (or "thermal") velocity for each particle.

total mass (of N particles, with mass 
$$m_i$$
):  $M = \sum_{i=1}^{N} m_i$ , (1)

CM of N particles, with a set of coordinates 
$$x_i$$
:  $M\mathbf{x}_0 = \sum_{i=1}^{N} m_i \mathbf{x}_i$ , (2)

CM velocity (of N particles, with velocity 
$$\dot{\mathbf{x}}_i$$
):  $M\dot{\mathbf{x}}_0 = \sum_{i=1}^N m_i \dot{\mathbf{x}}_i$ , (3)

Peculiar velocity of particle *i*, (momentum 
$$p_i = m_i u_i$$
):  $\mathbf{u_i} = \dot{\mathbf{x}}_i - \dot{\mathbf{x}}_0$ ,  $\sum_{i=1}^{N} m_i \mathbf{u}_i = 0$  (4)

Kinetic energy (T = temperature): 
$$K(\{\mathbf{p}\}) = \sum_{i=1}^{N} \frac{1}{2} m_i |\mathbf{u}_i|^2 = \sum_{i=1}^{N} \frac{|\mathbf{p}_i|^2}{2m_i} = \frac{3}{2} NkT.$$
 (5)

Potential energy: 
$$\Phi(\{\mathbf{x}\})$$
,  $\mathbf{F}_i = -\frac{\partial \Phi}{\partial \mathbf{x}}$ ,  $(\mathbf{F}_i = \text{force on a particle } i)$  (6)

Phase-space point (in 
$$\mathbb{R}^{6N+1}$$
):  $\Gamma = (\{\mathbf{x}\}, \{\mathbf{p}\}, \xi),$  (7)

Total energy: 
$$E = K(\{\mathbf{p}\}) + \Phi(\{\mathbf{x}\}) + E_{\xi}(\xi),$$
 (8)

where  $\{\mathbf{x}\} \equiv (\mathbf{x}_1, \dots, \mathbf{x}_N) \in \mathbb{R}^{3N}, \{\mathbf{p}\} \equiv (\mathbf{p}_1, \dots, \mathbf{p}_N) \in \mathbb{R}^{3N}, E_{\xi}(\xi) = \frac{3}{2}NkT_0\tau^2\xi^2$  is the heat-bath energy penalty for Nosé–Hoover thermostatting, here k is Boltzmann's constant, and  $T_0$  is the average temperature and  $\xi$  is the thermostat rate. We can now introduce the Nosé–Hoover equations of motion for thermostatting the system (either "sample" or "reservoir" in the Demonic system):

$$\dot{\mathbf{x}}_i = \mathbf{u}_i + \dot{\mathbf{x}}_0 \tag{9}$$

$$\dot{\mathbf{u}}_i = \frac{\mathbf{F}_i}{m_i} - \xi \mathbf{u}_i \tag{10}$$

$$\dot{\xi} = \frac{1}{\tau^2} \left[ \frac{T}{T_0} - 1 \right],\tag{11}$$

where  $\tau$  is collision time. We can then compute the rate of change of total, dE/dt = dQ/dt - dW/dt, for the NH thermostatted computational box, where Q is the heat injected into the system from the thermostat heat bath, and W is the work done by the system on its surroundings (e.g.,

work done to shear the fluid, or lift a weight, or change pressure or volume, etc.). From this, we can find the rate of change in the entropy, S, namely, dS/dt.

$$\dot{E} = \dot{K} + \dot{\Phi} + \dot{E}_{NH} = \dot{Q} - \dot{W}, \ \dot{Q} = T_0 \dot{S}, \ (\text{assuming that } x_0 \equiv 0)$$

$$\dot{K} + \dot{\Phi} = \sum_{i} \left( m_i \mathbf{u}_i \cdot \dot{\mathbf{u}}_i + \frac{\partial \Phi}{\partial \mathbf{x}_i} \cdot \mathbf{u}_i \right)$$
(12)

$$= \sum_{i} \left[ m_{i} \mathbf{u}_{i} \cdot \left( \frac{\mathbf{F}_{i}}{m_{i}} - \xi \mathbf{u}_{i} \right) - \mathbf{F}_{i} \cdot \mathbf{u}_{i} \right]$$

$$= -\xi \sum_{i} m_i |\mathbf{u}_i|^2 = -3NkT\xi \tag{13}$$

$$\dot{E} = -3NkT_0\tau^2\xi\dot{\xi} = -3NkT_0\tau^2\xi\left(\frac{T}{T_0} - 1\right) = -3NkT\xi - 3NkT_0\xi\tag{14}$$

Thermostatting only, i.e., 
$$\dot{W} \equiv 0 \implies \dot{E} = -3NkT_0\xi = T_0\dot{S}$$
 (15)

$$\Rightarrow \dot{S} = -3Nk\xi \tag{16}$$

The NVT temperature fluctuation  $\sigma_T/T_0 = [2/(3N)]^{1/2}$  is derived in Appendix A (as in Ref.<sup>6</sup>). The equations of motion (with initial CM velocity = 0) can be integrated by Størmer finite centered differences, where coordinates and the heat-flow variable are evaluated at integral values of the time step (as are forces, which depend on coordinates) while velocities are staggered by half time steps (as is the temperature). These centered difference equations of motion are time-reversible and avoid introducing center-of-mass drift errors, as well as systematic time-step errors (see details in Appendix B).

At equilibrium, long-time averages are equivalent to ensemble averages; for the nonequilibrium steady state (NESS), time averages are the whole game. (For the Gaussian distribution of the thermostatting coefficient and its number-dependence, see Appendix A)

Long-time averages at equilibrium (or NESS):

$$\langle T \rangle = \lim_{t \to \infty} \frac{1}{t} \int_0^t ds \, T(s) = T_0, \tag{17}$$

$$\langle \dot{T} \rangle = \lim_{t \to \infty} \frac{1}{t} \int_0^t ds \, \dot{T}(s) = \lim_{t \to \infty} \frac{T(t) - T(0)}{t} = 0, \tag{18}$$

At equilibrium, 
$$\langle \xi \rangle = 0$$
, (19)

$$\sqrt{\langle \xi^2 \rangle} = \frac{1}{\sqrt{3N} \cdot \tau} \quad \text{(Gaussian distribution)} \tag{20}$$

T and  $\xi$  are independent under Nosé–Hoover thermostatting:

$$\langle T\xi \rangle = T_0 \left[ \langle \xi \rangle + \tau^2 \langle \xi \cdot \dot{\xi} \rangle \right] = \langle T \rangle \langle \xi \rangle, \tag{21}$$

since 
$$\langle \xi \cdot \dot{\xi} \rangle = \left\langle \frac{d}{dt} \left( \frac{1}{2} \xi^2 \right) \right\rangle = 0$$
 (22)

Now, we are prepared to take these foundational concepts of NH thermostatting and generalize them to the two-state nonequilibrium heat-flow problem addressed by the Maxwell Demon<sup>5</sup>. NESS long-time averages of temperature, energy, and entropy are related to long-time averages of the two thermostat variables:

$$\langle \dot{E} \rangle = -3Nk \langle T_0 \rangle \langle \xi_0 \rangle - 3Nk \langle T_1 \rangle \langle \xi_1 \rangle = -3Nk T_0 \langle \xi_0 \rangle - 3Nk T_1 \langle \xi_1 \rangle \tag{23}$$

Nonequilibrium steady state requires:

$$\langle \dot{E} \rangle = 0 \quad \Rightarrow \quad \langle \xi_1 \rangle = -\frac{T_0}{T_1} \langle \xi_0 \rangle < 0$$
 (24)

Using entropy rates:

$$\langle \dot{E} \rangle = \langle \dot{Q}_0 \rangle + \langle \dot{Q}_1 \rangle = T_0 \langle \dot{S}_0 \rangle + T_1 \langle \dot{S}_1 \rangle \tag{25}$$

$$\langle \dot{S}_0 \rangle = -3Nk \langle \xi_0 \rangle, \quad \langle \dot{S}_1 \rangle = -3Nk \langle \xi_1 \rangle$$
 (26)

$$\therefore \quad \langle \dot{S} \rangle = \langle \dot{S}_0 \rangle + \langle \dot{S}_1 \rangle = -3Nk \left[ \langle \xi_0 \rangle + \langle \xi_1 \rangle \right]$$

$$=3Nk\langle \xi_0\rangle \left(\frac{T_1-T_0}{T_1}\right)<0, \tag{27}$$

which means the phase space contracts and its dimension becomes less than 6N + 1 for both sample and reservoir.

Clearly, the entropy never becomes steady, but drops forever as the phase-space distribution collapses onto a fractal strange attractor of lower dimensionality. The hot thermostat variable's long-time average is smaller in magnitude than the cold ( $|\xi_1| < \xi_0$ ), by virtue of the conservation of energy. From the equation for the rate of entropy change in the combined system (hot and cold), we see that entropy continues to get more and more negative in steady-state heat flow, which thereby demonstrates conclusively that it is easier to heat a sample than to cool it. (An alternative derivation of this nonequilibrium behavior of the entropy rate of change can be gotten from the Liouville continuity equation for the phase-space distribution function; see Appendix C)

The relationship of these NEMD heat-flow simulations to the Ibáñez lab experiments is clear, though the data from the NEMD thermostatting coefficients might have an analogue in steady-state

laboratory experiments: if the experimental power required to keep the two temperature regions at their respective temperatures were measured, they might show a bias similar to the absolute value of the NEMD thermostatting coefficients.

The heat flow results of NEMD in a three-dimensional multi-particle NH thermostatted fluid can be compared to a much simpler two-dimensional model of a single particle moving in a periodic cell, with temperature in the two directions thermostatted – one direction hot (x) at temperature  $T_1 = T_x$  and one cold (y) at  $T_0 = T_y$ . The statistical mechanics analysis presented here for both 2D N = 1 and 3D N >> 1 computer simulations give identical predictions about entropy rate and ease of heating compared to cooling.

#### II. RESULTS

## A. Revisiting Evans–Holian Results on the $\xi$ -distribution at Equilibrium: Asymmetry?

Reflecting upon the Maxwell Demon hot-and-cold simulations and considering the striking findings of asymmetry at equilibrium by Evans and Holian<sup>2</sup>, as well as thinking about the lessons learned from the simple cell model, where the equilibrium distribution of the thermostatting coefficient was perfectly symmetric and Gaussian, we thought it would be important to do a modern MD simulation, under Nosé-Hoover dynamics, of a fluid of N=32 particles interacting by the Lennard-Jones (LJ) soft-sphere potential  $\phi(r)=4\varepsilon\left(\frac{\sigma}{r}\right)^{12}$  with cutoff  $r_c=1.5\sigma$  (where  $\varepsilon$  is the depth of energy well for the full Lennard-Jones potential, and  $\sigma$  is its vdW radius or zero-energy crossing point). We repeated their trajectory of length t=120 (in LJ units, where  $\varepsilon=\sigma=m=k=1$ ), using a time-step  $\Delta t=0.003$  and thermostat relaxation (or collision) time  $\tau=0.09622$ . Moreover, we did extended simulations in both trajectory length and system size: N=32,  $t=1.2\times10^5$ ,  $\Delta t=0.003$  (small system, longer trajectory); N=1000,  $t=1.2\times10^5$ ,  $\Delta t=0.001$  (large system, longer trajectory).

Why re-do this old work? We needed to assure ourselves that the earlier work did not have some kind of systematic error, either some kind of inaccuracy in the integration of the equations of motion, or possible failure to maintain zero CM velocity, or the possible existence of finite system-size effects, or too short sampling times along the trajectory. We needed to perform the thermostat variable's distribution and assess for ourselves the error bars, by doing the error analysis in two different ways. Hence, the old and new system sizes and trajectory lengths, not to mention

careful centered-difference integration of the Nosé–Hoover thermostatting equations of motion, were deemed to be necessary for a definitive test of asymmetry – or not – at equilibrium.

To overlay data from larger systems, we rescale the horizontal axis of the thermostat distribution for N=1000 by a factor of  $\sqrt{1000/32}\approx 5.6$ , such that all curves can be meaningfully plotted together. This scaling arises from the Gaussian distribution of the variance of  $\xi:\langle\xi^2\rangle=1/(3N\tau^2)$  (see Appendix A). Figure 1 shows the probability distributions  $P(\xi)$  for all three cases. In the short trajectory that reproduces their original setup, the distribution appears Gaussian and centered at  $\langle\xi\rangle=0$ , in contrast to the skewed histogram reported in Figure 1 (Ref.<sup>2</sup>). We also confirmed that extending the trajectory length does not introduce any bias in  $\langle\xi\rangle$ . Both long simulations, with N=32 and N=1000, show symmetric, zero-mean Gaussian distributions. We also overlay the theoretical Gaussian curve corresponding to  $\xi\sim\mathcal{N}(0,\sigma_{\xi}^2)$ . The good agreement between the histograms and the theoretical curve confirms that the friction coefficient,  $\xi$ , behaves as a Gaussian random variable at equilibrium. For a discussion of our two methods of error estimation in MD simulations, see Appendix D.

In our implementation, the Nosé–Hoover thermostat acts only on the particles' peculiar velocities, ensuring zero initial CM velocity remains zero. The original 1985 setup may not have enforced this constraint correctly, nor can we be sure that the Størmer integration was done like Appendix B, so that slight asymmetries might have been introduced into their results. We emphasize that enforcing CM conservation and Størmer finite difference ensures proper sampling within the NH thermostatted ensemble.

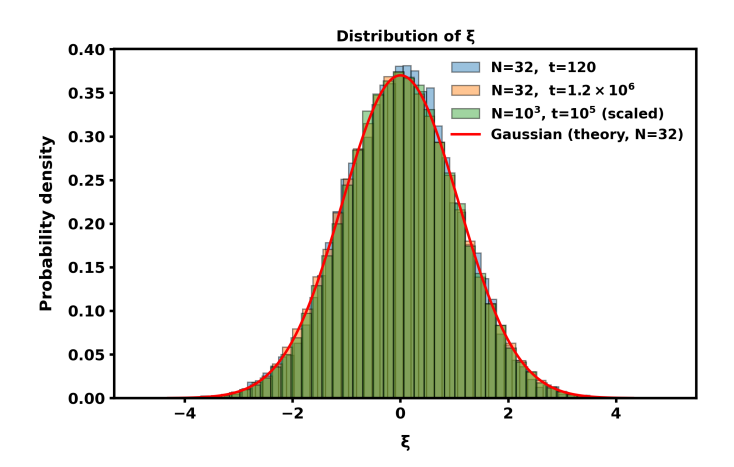


FIG. 1. Distribution of thermostat variable  $\xi$  for LJ systems. Distributions for N = 32, t = 120 (short),  $t = 1.2 \times 10^5$  (long), and N = 1000 long trajectory are shown. All distributions are symmetric about zero.

## B. Nonequilibrium Asymmetry in the Thermostatted Two-Temperature Cell Model

To investigate the statistical behavior of Nosé–Hoover thermostats under nonequilibrium conditions, we used the results of our recent study of a two-dimensional cell model with independent thermostats<sup>4</sup> applied along the x and y directions. The extended thermostat variables  $\xi_x$  and  $\xi_y$  are tracked in both equilibrium and NESS. Figure 2 shows the histograms of  $\xi_x$  and  $\xi_y$  for two cases, equilibrium:  $T_x = T_y = 0.5$  ( $\delta = T_x - T_y = 0.0$ ), and nonequilibrium:  $T_x = 0.5$ ,  $T_y = 0.05$  ( $\delta = 0.45$ ). In equilibrium, both thermostat variables are symmetrically distributed around zero with negligible skewness, as expected from time-reversible dynamics. Under nonequilibrium conditions, the distributions become highly asymmetric, with clear shifts in the mean and median values. These results are shown in Table I.

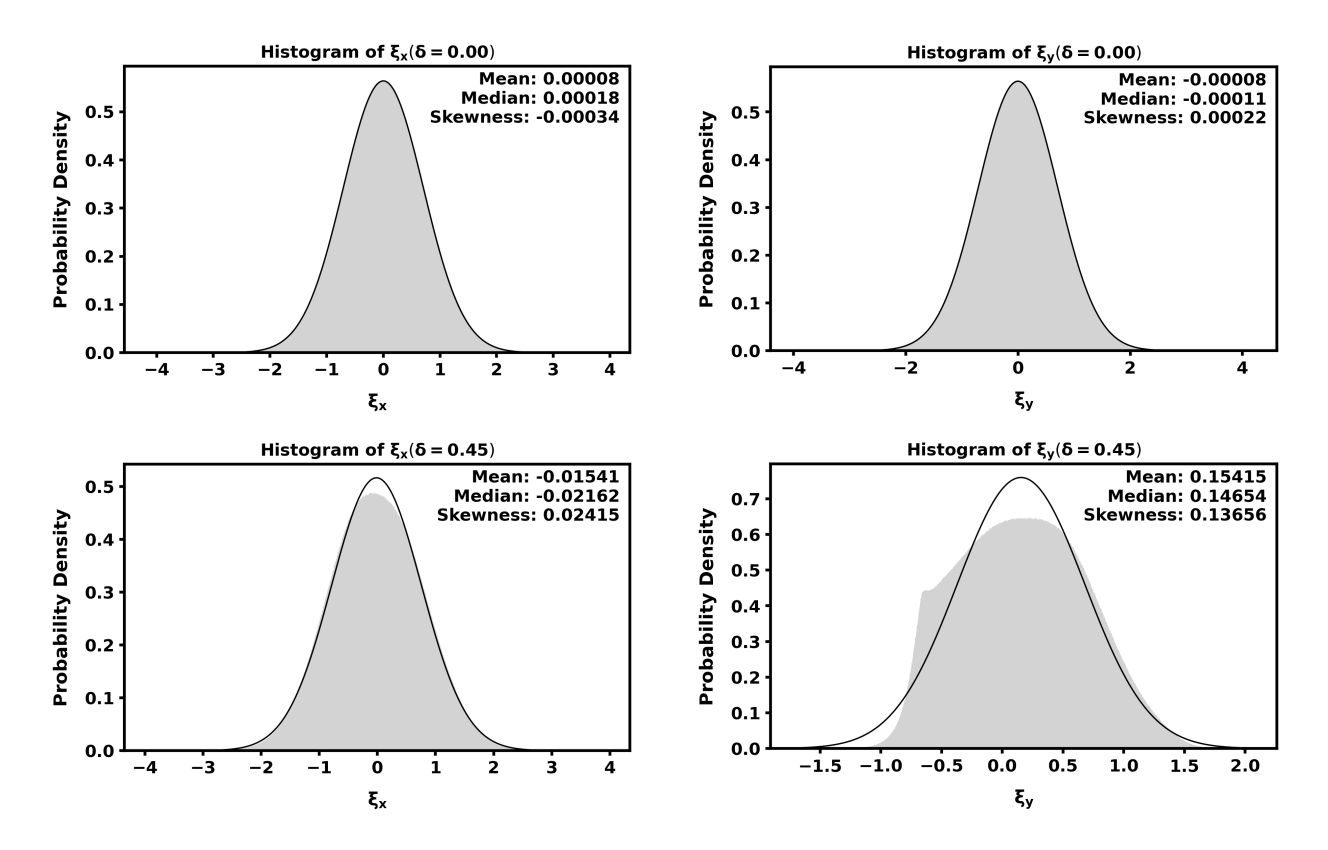


FIG. 2. Distributions of  $\xi_x$  and  $\xi_y$  in the two-temperature cell model. In equilibrium ( $\delta = 0$ ), both variables are centered around zero. Under nonequilibrium conditions ( $\delta = 0.45$ ), the thermostat variables develop strong asymmetry. The cold bath requires significantly stronger damping effort ( $\xi_y \gg \xi_x$ ) to maintain the steady-state energy flow.

In NESS, we observe  $\langle \xi_x \rangle < 0$  implies heating along x and  $\langle \xi_y \rangle > 0$  implies cooling along y. This

TABLE I. Mean and median values of  $\xi_x$  and  $\xi_y$  in equilibrium and NESS.

Case	Variable	Mean	Median
Equilibrium ( $\delta = 0.00$ )	$\xi_x$	+0.00008	+0.00018
	$\xi_y$	-0.00008	-0.00011
Nonequilibrium ( $\delta = 0.45$ )	$\xi_x$	-0.01541	-0.02162
	$\xi_y$	+0.15415	+0.14654

reflects the imposed thermal gradient: heat flows from the hot direction (x) to the cold direction (y), and the thermostats respond accordingly. Interestingly, the thermostat effort is highly asymmetric, explained analytically by the balance equation for steady-state energy input and output, outlined in our Maxwell Demon scenario.

The thermostat along the cold direction (y) must apply an order-of-magnitude stronger damping force to absorb the incoming energy flux, while the hot direction (x) requires only mild anti-damping to inject energy. The results obtained here are in good agreement with both equilibrium and nonequilibrium cases of the many-body simulations as substantiated by the statistical mechanical arguments we present in this paper. Thus, the heating is easier to accomplish than cooling, confirming at the atomistic level the lab experimental results of Ibáñez et al.<sup>1</sup>.

## III. CONCLUSION

We have demonstrated at the microscopic scale, by many-body molecular dynamics computer experiments and a very simple, but incredibly instructive single-particle two-dimensional cell model<sup>4</sup>, that true asymmetry between heating and cooling arises not in equilibrium, but in driven nonequilibrium steady states. The theory that allows us to quantify the rates was first outlined in earlier MD simulations of thermostatted side-by-side hot-and-cold regions<sup>5</sup>. By itself, this theory should have alerted us, two decades ago, to the inescapable fact of nonequilibrium heating/cooling asymmetry.

Prompted by lab experiments on asymmetric heating and cooling rates<sup>1</sup> we have revisited and resolved a discrepancy in the statistical behavior of the Nosé–Hoover thermostat first reported by Evans and Holian in 1985. While their original equilibrium simulations appeared to show a skewed distribution for the thermostat variable  $\xi$ , our modern simulation under identical initial

conditions included correct treatment of center-of-mass velocity, careful finite-difference integration of the equations of motion, and long-time sampling. The results reveal that the thermostat rate variable exhibits a totally symmetric Gaussian distribution, in agreement with equilibrium theory. We validated the mean-zero character of the distribution using two independent error estimation methods. We emphasize that symmetry is an equilibrium property.

In a two-temperature Nosé–Hoover one-particle cell model<sup>4</sup> with  $T_x > T_y$ , that is, nonequilibrium conditions, the mean thermostat variables become asymmetric, depending on the degree of deviation from linear response theory: we find that  $\langle \xi_y \rangle$  can become up to an order of magnitude larger than  $\langle \xi_x \rangle$ , matching the imposed temperature ratio. This asymmetry is explained analytically by a steady-state energy balance, leading to the relation  $\langle \xi_x \rangle / \langle \xi_y \rangle = -T_y/T_x$ .

Together, these findings clarify the nonequilibrium conditions under which thermostat asymmetry emerges and offer a microscopic explanation for recent experimental observations of unequal heating and cooling rates<sup>1</sup>. We have shown that Nosé–Hoover friction variables not only regulate energy exchange but also encode the thermodynamic structure of nonequilibrium states, including the chaotic phase-space contraction to a lower-dimensional, fractal, strange attractor. Moreover, our computer experiments have demonstrated relevance to real-world lab experiments. As a wise old cowboy once said, "When you're riding your horse, always be prepared for the unexpected." We observe that the same applies to nonequilibrium systems.

#### DATA AVAILABILITY STATEMENT

All results are based on direct numerical simulations from equations fully specified in the manuscript. No external datasets were generated or analyzed.

## **Appendix A: Derivation of NVT Thermal Fluctuation**

In this Appendix, we derive the canonical temperature fluctuation under Nosé-Hoover thermostatting. The NVT equilibrium canonical ensemble (N particles in volume V, and temperature T) is characterized by the phase-space distribution function  $\rho(\Gamma)$  at the 6N+1 dimensional phase point  $\Gamma = \{\mathbf{x}, \mathbf{y}, \xi\}$  which is the collection of 3N coordinates  $\mathbf{x}$ , 3N momenta  $\mathbf{p}$ , and the NH thermostat heat-flow variable  $\xi$ :  $\rho(\Gamma) = \exp(-\beta E)/Q_{NVT}$ , where  $\beta = 1/kT_0$ , k is Boltzmann's constant,  $T_0$  is the canonical-ensemble temperature set by the NH thermostat,  $E = K + \Phi + E_{\xi}$ , is the total

energy in the exponential Boltzmann factor the usual internal energy – the usual internal energy, kinetic K and potential  $\Phi$ , plus a harmonic thermostat energy,  $E_{\xi}=3/2~NkT_0\tau^2\xi^2$ , representing the NH heat bath<sup>6</sup>, and  $Q_{NVT}$  is the canonical partition function, the integral of the Boltzmann factor over all of phase space. Since  $\rho(\Gamma)=1/\Omega$ , where  $\Omega$  is the number of microstates for the system at  $\Gamma$ , the entropy of the system is  $S=-k\ln\rho=k\ln\Omega$  (Boltzmann's epitaph on his tomb in Vienna).

We can define the dimensionless thermostat strength, characterizing the exchange of energy between the NH heat bath and the N sample particles, as  $\zeta = \xi \tau$ , where  $\zeta$  is the thermostatting rate variable and  $\xi$  is the thermostat relaxation time (most efficiently chosen as the collision time). Then, the harmonic heat-bath "potential" is  $E_{\xi} = (1/2)\kappa\zeta^2$  where  $\kappa = 3NkT_0$  is the "force constant" or "stiffness" of the thermostatting potential well. If either  $\zeta > 0$  (so that friction takes kinetic energy out of the 3N particle momenta by slowing them down) or if  $\zeta < 0$  (so that antifriction pumps energy into the momenta, speeding them up) – in either case – there is an energetic penalty for thermostatting added to the 6N+1-dimensional total energy of system. The phase-space distribution function contribution from the NH heat bath  $\zeta$  ends up being a simple Gaussian:  $\exp(-\beta E_{\xi}) = \exp(-3N\zeta^2/2)$ , whereby the variance of the dimensionless thermostatting strength is  $\zeta(\zeta) = 1/(3N)$ . Hence, the ensemble average (or time average) is  $\zeta(\zeta) = (1/2)\kappa\zeta(\zeta) = kT_0/2$ , which is a factor of 3N smaller than the particle momentum contribution to the kinetic energy:  $\zeta(\zeta) = 3N(kT_0/2)$ . For a monatomic harmonic crystalline solid,  $\zeta(\zeta) = \zeta(\zeta) = \zeta(\zeta)$  so that each of the  $\zeta(\zeta) = 3N(kT_0/2)$  are a monatomic harmonic fluids fall in between these two idealized limits.

The whole idea of thermostatting is to approach the NVT thermodynamic limit long before N becomes infinite, at which point, the NH thermostat contributes nothing to the system.

Finally, the temperature (thermal) fluctuation,  $\sigma_T^2$ , is obtained by noticing that the phase space can be separated into independent partition functions governing  $\mathbf{x}$ ,  $\mathbf{p}$ , and  $\boldsymbol{\xi}$ , and evaluating ensemble averages within them.

$$E = K(\mathbf{p}) + \Phi(\mathbf{x}) + E_{\xi}(\xi)$$

Independent phase spaces:

$$\begin{split} Q_{NVT}(\Gamma) &= \int d\Gamma \exp\left(-\beta E(\Gamma)\right) = Q_{k}(\mathbf{p}) \ Q_{\Phi}(\mathbf{x}) \ Q_{\xi}(\xi), \\ \text{e.g.,} \quad Q_{k} &= \int d\mathbf{p} \ \exp\left(-\beta K(\mathbf{p})\right), \\ \langle K \rangle &= \frac{3}{2}Nk\langle T \rangle \frac{\text{Using } \langle T \rangle = T_{0}}{2} \frac{3}{2}NkT_{0} \\ &= \frac{1}{Q_{K}} \int d\mathbf{p} \ K \exp\left(-\beta K\right) = -\frac{1}{Q_{K}} \frac{\partial}{\partial \beta} \int d\mathbf{p} \ \exp\left(-\beta K\right) \\ &= -\frac{1}{Q_{K}} \frac{\partial Q_{K}}{\partial \beta}. \\ \langle K^{2} \rangle &= \frac{1}{Q_{K}} \int d\mathbf{p} \ K^{2} \exp\left(-\beta K\right) = -\frac{1}{Q_{K}} \frac{\partial}{\partial \beta} \int d\mathbf{p} \ K \exp\left(-\beta K\right) \\ &= -\frac{1}{Q_{K}} \left[ \frac{\partial Q_{K}}{\partial \beta} \cdot \langle K \rangle + Q_{K} \frac{\partial \langle K \rangle}{\partial \beta} \right] = \langle K \rangle^{2} + kT_{0}^{2} \frac{\partial \langle K \rangle}{\partial T_{0}} \\ &= \langle K \rangle^{2} + \frac{3}{2}Nk^{2}T_{0}^{2}. \\ \sigma_{K}^{2} &= \langle K^{2} \rangle - \langle K \rangle^{2} = \frac{3}{2}Nk^{2}T_{0}^{2} = \left(\frac{3}{2}Nk^{2}\right) \left(\langle T^{2} \rangle - \langle T \rangle^{2}\right). \end{split}$$

Thus,  $\sigma_T/T_0 \sim 1/\sqrt{N}$ , which vanishes in the thermodynamic limit.

## Appendix B: Nosé-Hoover Equations of Motion on the Computer

Nosé–Hoover equations of motion (with initial CM velocity = 0) can be integrated by Størmer finite centered differences<sup>6</sup>, where coordinates and the heat-flow variable are evaluated at integral values of the time step  $\delta$  (as are forces, which depend on coordinates) while velocities are staggered by  $\delta/2$  (as is the temperature):

 $\Rightarrow$   $\sigma_T^2 = (\langle T^2 \rangle - \langle T \rangle^2) = \frac{2}{3} \frac{T_0^2}{N}$ . (temperature fluctuation)

Suppressing particle indices i = 1:N, and vector notation  $\alpha = 1:3$ ,

$$\begin{aligned} x(t) &= x(t - \delta) + u(t - \frac{1}{2}\delta) \cdot \delta + O(\delta^3) \\ \xi(t) &= \xi(t - \delta) + \frac{1}{\tau^2} \left[ \frac{T(t - \frac{1}{2}\delta)}{T_0} - 1 \right] \cdot \delta + O(\delta^3) \end{aligned}$$

where from previous time-step,  $3NkT(t-\frac{1}{2}\delta) = \sum_{i}\sum_{\alpha}m_{i}u_{i\alpha}^{2}(t-\frac{1}{2}\delta)$ 

$$u(t+\frac{1}{2}\delta) = \frac{u(t-\frac{1}{2}\delta)[1-\frac{1}{2}\xi(t)\cdot\delta] + a(t)\cdot\delta}{1+\frac{1}{2}\xi(t)\cdot\delta} + O(\delta^3).$$

where from previous time-step, a(t) = F[x(t)]/m (Newton: F = ma)

The local error in the coordinate, velocity, and thermostat variable equations of motion is third order, i.e., the Taylor series terms in  $\delta^3$  and higher have been excluded in the finite difference equations above. The global error,  $\delta^4$  is obtained by integrating the coordinate one more time (to  $t + \delta$ ), substituting the velocity from the previous half-time step, and rearranging to get the central difference acceleration and velocity, which are time-reversible:

$$a(t) - \xi(t)u(t) = \frac{x(t+\delta) - 2x(t) + x(t-\delta)}{\delta^2} + O(\delta^2),$$

$$u(t) = \frac{x(t+\delta) - x(t-\delta)}{2\delta} + O(\delta^2)$$
(B1)

When  $\delta > 0$ , time marches forward, and when  $\delta < 0$ , time goes backward.

# Appendix C: Derivation of nonequilibrium entropy change from Liouville equation

Liouville continuity equation for phase space distribution function  $\rho(\Gamma,t)$ :

$$\frac{\partial \rho}{\partial t} + \frac{\partial}{\partial \Gamma} \cdot \dot{\Gamma} \rho = 0 = \frac{d\rho}{dt} + \rho \Lambda$$
$$\frac{d\rho}{dt} = \frac{\partial \rho}{\partial t} + \dot{\Gamma} \cdot \frac{\partial \rho}{\partial \Gamma},$$
$$\Lambda = \frac{\partial}{\partial \Gamma} \cdot \dot{\Gamma} = -\frac{d}{dt} \ln \rho$$

$$\Lambda = \sum_{\alpha} \left( \frac{\partial \dot{x}_{i\alpha}}{\partial x_{i\alpha}} + \frac{\partial \dot{p}_{i\alpha}}{\partial p_{i\alpha}} + \frac{\partial \dot{\xi}_{0}}{\partial \xi_{0}} + \frac{\partial \dot{\xi}_{1}}{\partial \xi_{1}} \right)$$
$$= \sum_{\alpha} \left( \frac{\partial \dot{p}_{i\alpha}}{\partial p_{i\alpha}} \right) = -3N(\xi_{0} + \xi_{1})$$

Finally, using the standard entropy definition:

$$\langle \dot{S} \rangle = -k \frac{d}{dt} \langle \ln \rho \rangle = k \langle \Lambda \rangle = -3Nk \left[ \langle \xi_0 \rangle + \langle \xi_1 \rangle \right]$$

#### **Appendix D: Error Analysis**

#### 1. Standard Error of the Mean

The standard error of the mean, e.g., for the thermostat variable, is estimated from:

$$\sigma_{mean} = rac{\sigma}{\sqrt{N_{eff}}},$$

where  $\sigma$  is the sample standard deviation, and  $N_{eff}$  is the effective number of statistically independent samples. In a time series with persistence over a characteristic timescale,  $\tau$ , (the mean correlation time, approximately the collision time – which also happens to be the usual best choice for the thermostat relaxation time),  $N_{eff} \approx t/\tau$ . This yields the standard error formula:

$$\sigma_{mean} = rac{\sigma}{\sqrt{t/ au}}.$$

This method is simple to implement, requires no auto-correlation or fitting analysis, and can be applied to any observable (e.g., energy, pressure, thermostat variables) using the same set of thermal zero-crossings.

## 2. Kinetic-Crossing Method

An alternative to estimating the standard error of the mean is the kinetic-crossing method (see Fig. 2 of  $^2$ ). This approach estimates the number of effectively independent samples in a Nosé–Hoover thermostatted trajectory by counting the number of times the instantaneous kinetic temperature, T(t), crosses its mean value,  $\langle T \rangle$ , assumed equal to the thermostat value,  $T_0$ , at equilibrium.

We define a zero-crossing whenever T(t) changes sign relative to  $T_0$ , between successive time steps, providing an estimate of the number of statistically independent fluctuations in the simulation. Assuming each crossing corresponds to an effectively uncorrelated sample, i.e.,  $n_{cross} \approx t/\tau$ , the standard error of the mean for an observable A can be estimated as:

$$\sigma_{cross} = \frac{\sigma_A}{\sqrt{n_{cross}}}$$

where  $\sigma_A$  is the standard deviation of A over the trajectory.

We applied this method to estimate the uncertainty in the Nosé–Hoover friction coefficient,  $\xi$ , and compared it to the  $\tau$ -based estimate. In Table II, we summarize results for all three systems, N=32 short and run long runs, and N=1000. For N=32 systems we compare the standard error of  $(\xi)$  obtained via both the kinetic-crossing and the  $\tau$ -based methods and for N=1000 system we report that  $\tau$ -based estimate. The two estimates show good agreement. The results of our MD simulations of a many-body soft-sphere fluid at equilibrium, far from the melting line, were definitive: the distribution of the thermostatting coefficient is almost perfectly Gaussian, with zero mean and median, and with the theoretical thermal width. These results correct a long-standing misunderstanding in the behavior of the Nosé–Hoover thermostat and hold across both small and

large systems, with errors rigorously validated using two independent methods. We conclude that skewed distributions of  $\xi$  are not intrinsic to the thermostat and we are not sure what was the source of error in the Ref.<sup>2</sup> calculations.

TABLE II. Comparison of standard error of mean estimates of  $\xi$  using (i) kinetic-crossing N=32 systems and (ii) time-based methods for all systems.

N	time	$\Delta t$	SE <sub>crossing</sub>	$SE_{\tau ext{-based}}$
32	120	0.003	0.0031	0.0028
32	$1.2\times10^6$	0.003	0.00003	0.00003
1000	10 <sup>5</sup>	0.001	N/A	0.00002

#### **REFERENCES**

<sup>&</sup>lt;sup>1</sup>Miguel Ibáñez, Cai Dieball, Antonio Lasanta, Aljaž Godec, and Raúl A Rica. Heating and cooling are fundamentally asymmetric and evolve along distinct pathways. *Nature Physics*, 20:135–141, 2024.

<sup>&</sup>lt;sup>2</sup>DJ Evans and BL Holian. The Nose-Hoover thermostat. *Journal of Chemical Physics*, 83(8):4069–4074, 1985.

<sup>&</sup>lt;sup>3</sup>William G Hoover. Canonical dynamics: Equilibrium phase-space distributions. *Physical review A*, 31(3):1695, 1985.

<sup>&</sup>lt;sup>4</sup>Hesam Arabzadeh, Carol Griswold Hoover, William Graham Hoover, and Brad Lee Holian. Chaos in nonequilibrium two-temperature  $(T_x, T_y)$  Nosé-Hoover cell models, 2025. arXiv: 2507.10863

<sup>&</sup>lt;sup>5</sup>Simulations of vibrational relaxation in dense molecular fluids. II. Generalized treatment of thermal equilibration between a sample and a reservoir; Evaluating shear viscosity: Power dissipated versus entropy produced, *J. Chem. Phys.* **117**, 1173–1180, 9567–9568 (2002).

<sup>&</sup>lt;sup>6</sup>Brad Lee Holian, Arthur F Voter, and Ramon Ravelo. Thermostatted molecular dynamics: How to avoid the Toda demon hidden in Nosé-Hoover dynamics. *Physical Review E*, 52(3):2338, 1995.